



# High-entropy alloy coating deposition by detonation spraying combined with heat treatment

Igor Batraev<sup>1</sup> · Dina V. Dudina<sup>1</sup> · Denis K. Rybin<sup>1</sup> · Vladimir Yu. Ulianitsky<sup>1</sup> · Alexey Sova<sup>2</sup> · Ahmad Ostovari Moghaddam<sup>3</sup> · Maria Doubenskaia<sup>2</sup> · Evgeny Trofimov<sup>3</sup> · Marina Samodurova<sup>3</sup>

Received: 30 June 2023 / Accepted: 2 October 2023 / Published online: 18 October 2023  
© The Author(s), under exclusive licence to Springer-Verlag London Ltd., part of Springer Nature 2023

## Abstract

In this work, feasibility tests of new two-stage approach of deposition of thick high-entropy alloy coatings were performed. At the first stage of this approach, metal composite coating is formed by detonation spraying of low-entropy metal powder blends. At the second stage, the composite precursor coating is heat treated in order to promote the synthesis of high-entropy phases. The tests were carried out using three different powder mixtures of Fe, Ni, Cu, Co, and Al powders. Experimental results showed that the detonation spraying allows formation of uniform metal composite coating. The microstructure analysis and microhardness measurements of the coating before and after heat treatments confirmed that the heat treatment enables element diffusion in the coating followed by formation of CoFeNi, CoCuFe<sub>0.8</sub>Ni, and Al<sub>0.05</sub>CoCu<sub>0.3</sub>FeNi alloys with uniform *fcc* structure after recrystallization. At the same time, the final composition of the coatings differed from the targeted ones due to different deposition efficiencies of the particles during detonation spraying process.

**Keywords** Detonation spraying · High-entropy alloy · Composite coating · Heat treatment

## 1 Introduction

Deposition of coating from high-entropy alloys (HEA) is a new and rapidly expanding development direction of the thermal spray technologies. Nowadays, high-entropy metal alloys (HEA) are considered as materials with high application potential in different domains such as mechanical, chemical, aerospace, and automotive industries [1]. The concept of high-entropy alloys is based on the high value of mixing entropies of solid solution phases that improves the alloy stability in comparison with intermetallic phases, especially at high temperatures. Initially, the HEAs were defined as the alloys containing at least five principal elements, each having atomic percentage between 5 and 35% [1]. Nowadays, it is considered that only the alloys that form a solid

solution without intermetallic phases should be considered true high-entropy alloys, whereas the multiphase alloys containing five or more elements with high elemental percentage are called complex concentrated alloys [2].

At present, many articles presenting successful deposition of HEA coating by different thermal spray techniques like HVOF and HVAF [3–6], atmospheric plasma spray [7–9], detonation spray [10], and cold spray [11] are available. Analysis of mechanical properties and chemical stability of such coatings revealed extremely high application potential of these alloys.

However, it is important to note that in all these works, the HEA coatings were deposited using the previously prepared high-entropy alloy powders. The HEA powders are usually manufactured by gas atomization or ball-milling technique [3–11]. The main disadvantage of this approach is the low commercial availability of the HEA powders. Producing of HEA powder, especially with customized composition, is a complicated process with low production rate (in case of ball-milling process) and high cost. Thus, nowadays, only few types of HEA alloy powders for thermal spray are available on the market.

In this regard, the development of an approach allowing thermal spray deposition of high-entropy alloy coatings

✉ Alexey Sova  
sova.aleksey@gmail.com

<sup>1</sup> Lavrentyev Institute of Hydrodynamics SB RAS, Novosibirsk, Russia

<sup>2</sup> ECL-ENISE, LTDS Laboratory, UMR 5513, University of Lyon, Saint-Etienne, France

<sup>3</sup> South Ural State University, Chelyabinsk, Russia

without preliminary manufacturing of HEA powders could be interesting from an application point of view. The principle of such two-stage approach is schematically presented in Fig. 1. In the first stage of this hybrid technique, the metal composite coating is deposited by detonation spraying. It is important to note that in this stage, the mixture of low-cost low-entropy metal powders will be used. However, the final composition of the composite coating has to be closed to the desired composition of HEA. In the second stage, the coating heat treatment is applied in order to promote the element diffusion in the coating and create favorable conditions for formation of single solid solution in the coating using the elements of composite coatings as the precursors.

In our previous study, it was demonstrated that three-, four-, and five-component metal composite coatings with acceptable control of the coating elemental composition could be successfully deposited by detonation spraying [12]. As a result, the multimaterial coating consisting of inclusions of different metal particles could be formed. It is important to note that in case of successful development, this hybrid approach will allow manufacturing of HEA coatings with customized elemental compositions. Fine adjustment of precursor coating composition and optimization of heat-treatment procedure could potentially open the possibility to form HEA coatings with almost any combination of metallic elements.

The main purpose of this work was to perform the feasibility test of the proposed two-stage approach and to address the following questions:

- The metal composite coating deposited by detonation spray using powder mixtures with  $N$  components consist of melted and adhered particles with mean characteristic distance between the different particles equal to  $d \times N$  where  $d$  is the mean size of the particle. In case of deposition of five component coating, this distance could reach 150–200  $\mu\text{m}$  (Fig. 2). Would the elemental diffusion be induced in the precursor coating enough to

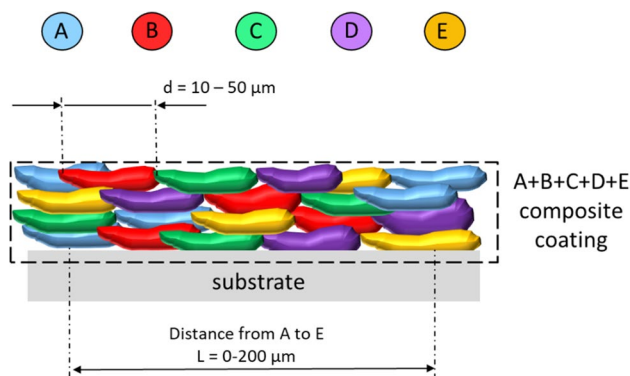
obtain good element mixing enabling formation of HEA phases?

- Application of heat treatment for element mixing and new HEA phase formation could potentially impact the coating integrity. Would it be possible to find the heat-treatment parameters sufficient for both phase transformation and coating integrity preserving?

It should be noted that the possibility of elaboration of HEA coating using hybrid approach combining the detonation spraying with following heat treatment has never been discussed in literature.

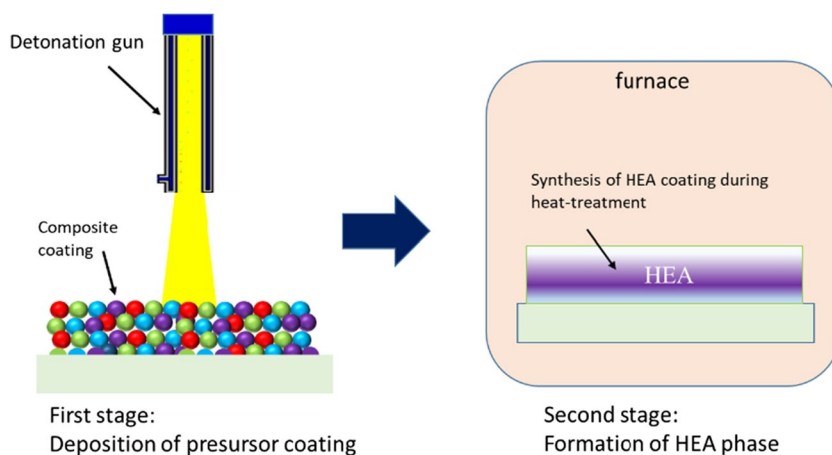
## 2 Materials and methods

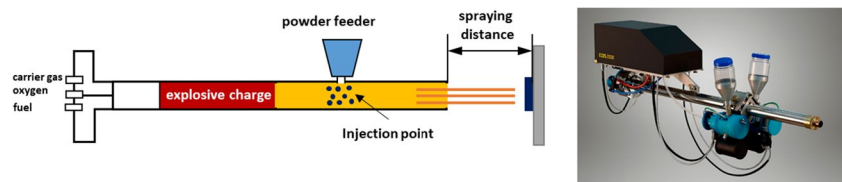
The coating deposition was performed using detonation spraying gun CCDS2000 developed at Lavrentyev Institute of Hydrodynamics SB RAS (Novosibirsk, Russia) [13–15]. The working principle of the gun is presented in Fig. 3. In the test, the barrel with 20 mm diameter and 1400 mm length was used. The powder injection point was set at 400



**Fig. 2** Spatial structure of detonation spraying metal composite deposited using the powder mixture of five powders

**Fig. 1** Schematics of two-stage approach of HEA coating deposition consisting of detonation spraying of precursor coating with following heat treatment



**Fig. 3** Schematics and overview of detonation gun CCDS2000

mm from the barrel outlet. The substrate was fixed at 100 mm distance after the barrel outlet. Coatings were deposited using “hot” spraying mode [12] corresponding to following process parameters: explosive mixture  $C_2H_2 + O_2$ , with the barrel filling ratio by explosive charge equal to 60%.

The particle in-flow parameters were calculated LIH code [13] also developed by the Institute of Hydrodynamics SB RAS for numerical simulation of detonation spraying process.

Spraying was performed on the mild-steel substrate sand-blasted prior to coating deposition. The substrate thickness was 3 mm.

The experiments were carried-out using three different single-element metal powder mixtures. In order to define the mixture compositions that could potentially lead to formation of high-entropy alloy phases after coating heat treatment, the thermodynamic and topological calculations were carried out. At present, many different physical criteria are used to predict the probability of single solid solution formation in high-entropy alloys [1, 14, 15]. The typical parameters mainly used for these calculations are mixing enthalpy  $\Delta H_{mix}$ , mixing entropy  $\Delta S_{mix}$ , and atomic size mismatch  $\delta$ . Zhang et al. [14] reported that single solid solutions could form in high-entropy alloys with parameters satisfying the criteria:  $-20 < \Delta H_{mix} < 5$  kJ/mol,  $12 < \Delta S_{mix} < 17.5$  J/K mol, and  $\delta < 6.4\%$ . Guo and Liu [15] found that solid solution is expected if all the three parameters meet the requirements of  $-22 < \Delta H_{mix} < 7$  kJ/mol,  $0 < \delta < 8.5$ , and  $11 < \Delta S_{mix} < 19.5$  J/K mol.

It was decided to perform the experiments with powders containing five elements: iron, copper, aluminum, cobalt, and nickel. These elements are often used in high-entropy alloys with *fcc*, *bcc*, and mixed structures [1]. To select elemental compositions, the mixing enthalpy, mixing entropy, and atomic size difference were calculated. The values of mixing enthalpies used for calculations are shown in Table 1.

The calculation allowed to determine three mixture candidates. The composition of powder mixtures and their enthalpy, entropy, and atomic size mismatch are presented in Table 2. The mixtures were prepared by weighing of pure metal powders using the laboratory scale with the 0.01-g precision. The composition of each powder was taken from the material datasheet provided by powder suppliers. One can see that the mixture with the mass composition with equal percentage of iron, nickel, and cobalt labeled as mix I meets the single solid solution

**Table 1** Chemical mixing enthalpies of the atomic pairs among the alloying elements (kJ/mol)

	Ni	Fe	Cu	Al	Co
Ni	0	-2	4	-22	0
Fe	-2	0	13	-11	-1
Cu	4	13	0	-1	6
Al	-22	-11	-1	0	-19
Co	0	-1	6	-19	0

formation criteria. The mixing enthalpy, mixing entropy, and atomic size mismatch of the third mixture mix III containing 5 elements also lays in the required range. The entropy and the atomic size mismatch of the mix II also satisfy the requirements, but its mixture enthalpy is higher than the criteria defined by Guo and Liu (9.99 kJ/mol vs. 7 kJ/mol).

The composition of mix I and mix II did not have direct industrial application and were used for feasibility test only. The composition of mix III powder blend could potentially lead to formation of  $Al_{0.05}Cu_{0.25}CoFeNi$  alloy having high application potential. It is known from the literature that the alloys of AlCuCoFeNi family have high wear-resistant and corrosion resistant properties [16–18] and could be used as a promising alternative to intermetallic and Stellite coatings used for wear and corrosion protection [19, 20].

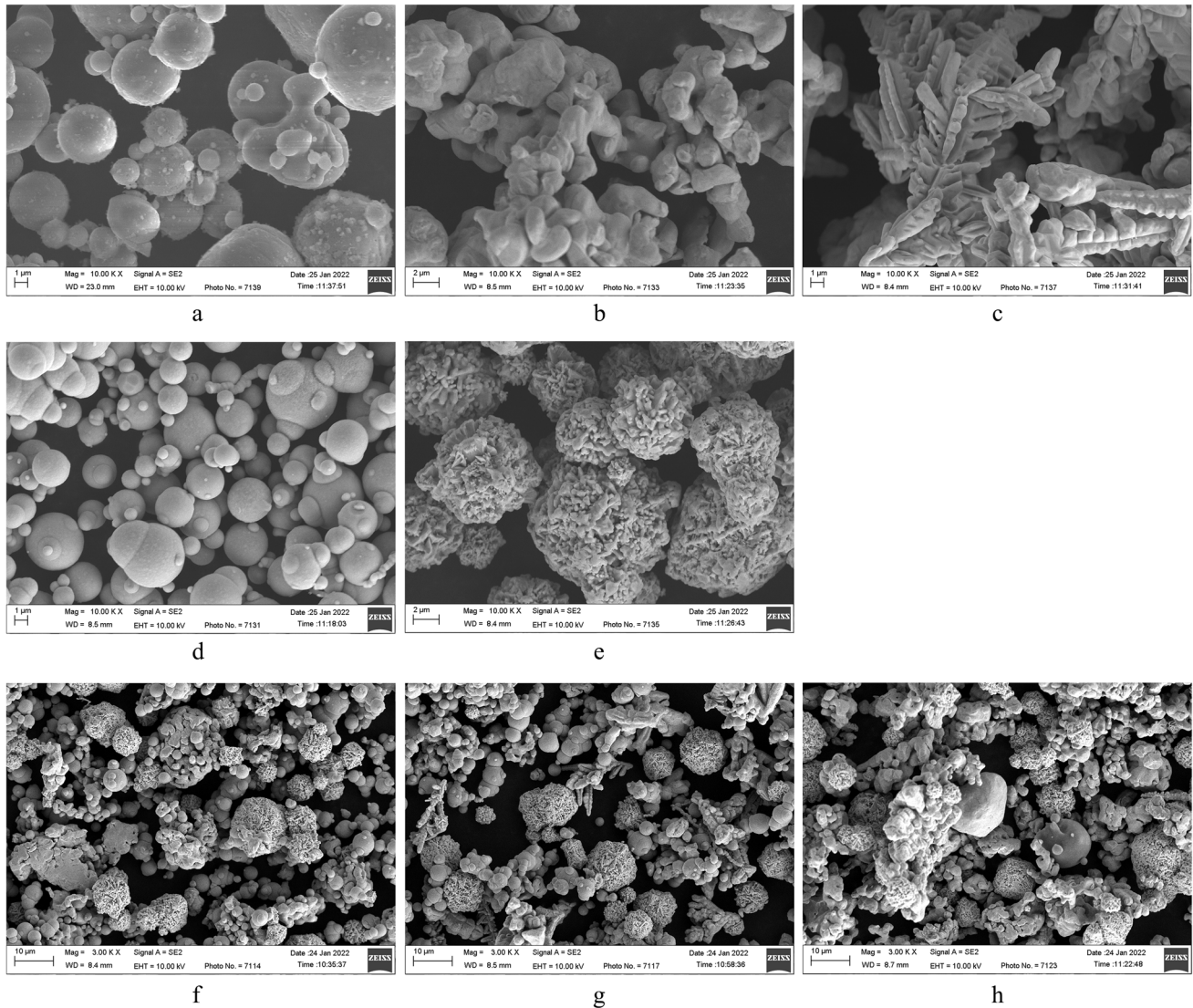
The powder mixtures were prepared using the rotating laboratory mixer with mixing time equal to 30 min. The SEM images of the powders and mixtures are presented in Fig. 4.

Heat treatment of coatings was performed in vacuum furnace with internal pressure equal to 10 Pa. The HT was carried out at 800 °C and 900 °C with treatment duration equal to 30 min with cooling down in furnace.

The X-ray diffraction (XRD) patterns of the powders and coatings were obtained by a D8 ADVANCE diffractometer (Bruker AXS, Germany) with Cu  $K\alpha$  radiation. The scanning electron microscope Hitachi-Tabletop TM-1000 (Japan) and scanning electron microscope Jeol JSM7001F equipped with energy-dispersive X-ray spectroscopy (EDS; Oxford INCA X-max 80) were applied for the analysis of the powder morphology and coating microstructure. The elemental composition of the coatings was calculated as the mean value from ten measurements taken from the square zones with dimensions  $150 \times 150$   $\mu$ m.

**Table 2** Elemental composition of the powder mixtures used for the precursor coating deposition

	Mix I 33% Fe + 33% Co + 33% Ni (atomic percent)	Mix II 25% Fe + 25% Co + 25% Ni + 25% Cu (atomic percent)	Mix III 30% Fe + 30% Co + 30% Ni + 8% Cu + 2% Al (atomic percent)
Al, wt%	0	0	0.9
Co, wt%	34.0	24.9	30.7
Cu, wt%	0	26.7	8.8
Fe, wt%	32.2	23.6	29.1
Ni, wt%	33.8	24.8	30.5
Enthalpy $\Delta H_{\text{mix}}$ , kJ/mol	-2.61	9.99	-0.25
Entropy $\Delta S_{\text{mix}}$ , kJ/mol	9.13	11.5	11.33
Atomic size mismatch $\delta$ , %	1.05	1.14	2.18

**Fig. 4** Powders used in experiments; **a** aluminum, **b** cobalt, **c** copper, **d** iron, **e** nickel, **f** mixture I, **g** mixture II, **h** mixture III

### 3 Results

#### 3.1 As-sprayed precursor composite coating

Prior to coating deposition, the calculation of particle parameters was performed. The simulation results are summarized in Fig. 5. Figure 5a clearly shows that under applied deposition parameters, the iron particles are on the melting shelf at the barrel outlet. Particles of cobalt, nickel, and copper are overheated inside the barrel to almost 2500 K. However, due to the sufficiently large loading depth (400 mm), they noticeably cool down in the rarefaction wave and fly out of the barrel with a temperature of about 2000 K, which is only 20% higher than their melting point. Light aluminum particles are almost instantly accelerated to the speed above 1000 m/s that limits the efficiency of gas-particle heat exchange due to low dwell time and low Nusselt number. As a result, the particle outlet temperature of aluminum does not exceed 1000 K. Thus, despite the strong difference in the thermophysical properties of the components of the powder mixture, it was possible to choose a deposition mode in which all components arrive on the substrate in molten state without

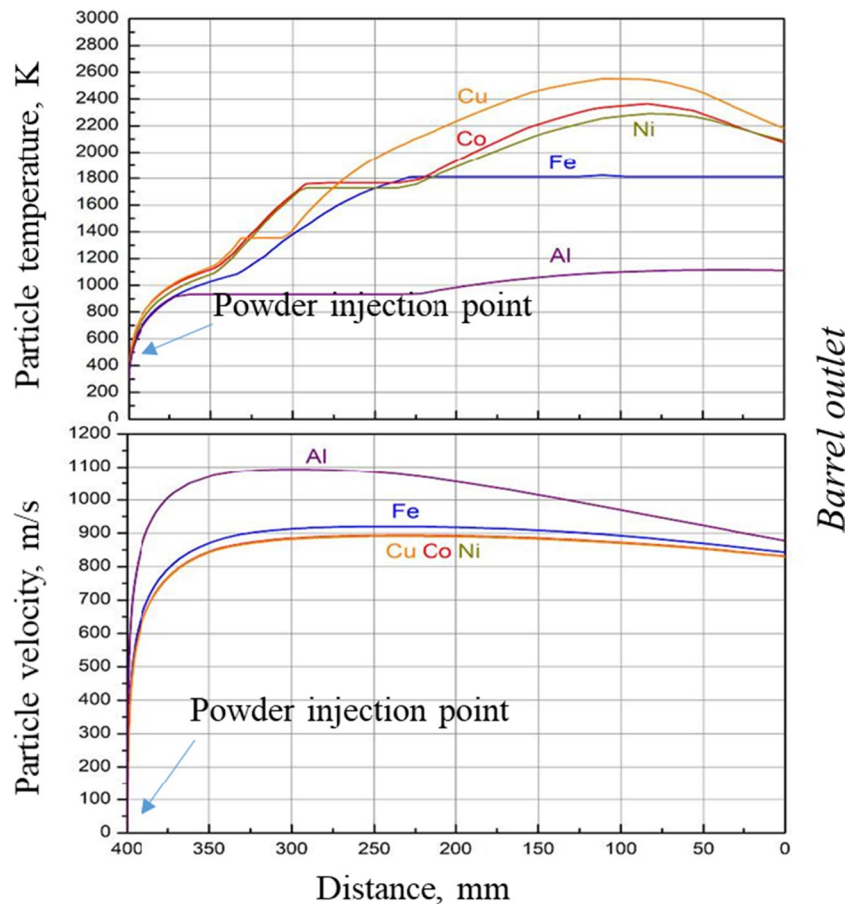
strong overheating and at almost the same speed of about 850 m/s (Fig. 5b). This provides the best conditions for the formation of a homogeneous composite.

For all three mixture compositions, the coatings were successfully deposited. The thickness of the coatings varied from 0.35 to 0.4 mm. The coating microstructures at low magnification are presented in Fig. 6. The low-magnification observation did not reveal significant defects in the coatings. The coating had dense structure. Some small pores at the interface between adhered particles were detected.

The results of SEM observations and of the EDS analysis are presented in Fig. 7. Obtained composite coatings had lamellae structure. One can see that all lamellas were flattened in the direction perpendicular to the impact direction. Thus, one can conclude that the particles impacted the surface in liquid state that is confirmed by numerical simulation results. Also, due to the liquid state impact, some limited mixing of materials at the lamellae peripheries is observed. At the same time, due to very high cooling rate, the material diffusion was limited and did not affect the main volume of particles.

The EDS analysis allowed estimation of the coating elemental composition and comparison with initial powder

**Fig. 5** Particle temperature and velocity evolution in the detonation gun barrel



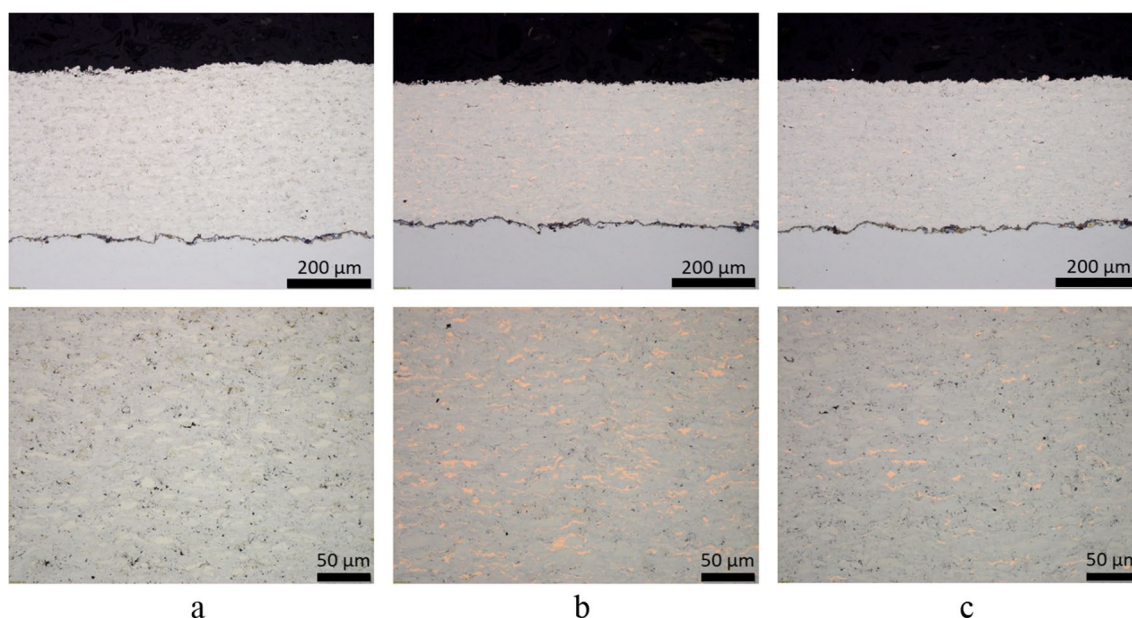


**Fig. 6** Optical images of the composite coating cross-sections deposited using mix I (a), mix II (b), and mix III (c) powder blends

mixture composition. The results of analysis are presented in Table 3.

The EDS analysis revealed some changes of the coating composition in comparison with the initial blend compositions (Table 3). In particular, the quantity of Fe in sprayed coatings was lower than initial ones. As a result, the amount of Cu, Ni, Co, and Al was increased. This difference could be explained by lower deposition efficient of the iron particles in comparison with other powders when spraying in mixture. Similar phenomenon was previously discussed in details in [12].

Changing of chemical composition of the coating relatively the initial mixture composition could affect the thermodynamic and topology parameters of the element mixing and shift the mixture out from the parametric window favorable for formation single solid solution of HEA. In order to verify if the mixing parameters in obtained precursor still favorable for formation of HEA during heat treatment, the mixing enthalpy, entropy, and atomic size mismatch were recalculated for the new ratio of elements (Table 3). Calculation showed that only the coating deposited using mix III powder blend meets the requirements defined by Guo and Liu [13] for formation of HEA with single solid solution. Nevertheless, the experiments with heat treatment were conducted for all three types of coatings.

### 3.2 Coating structure after heat treatments

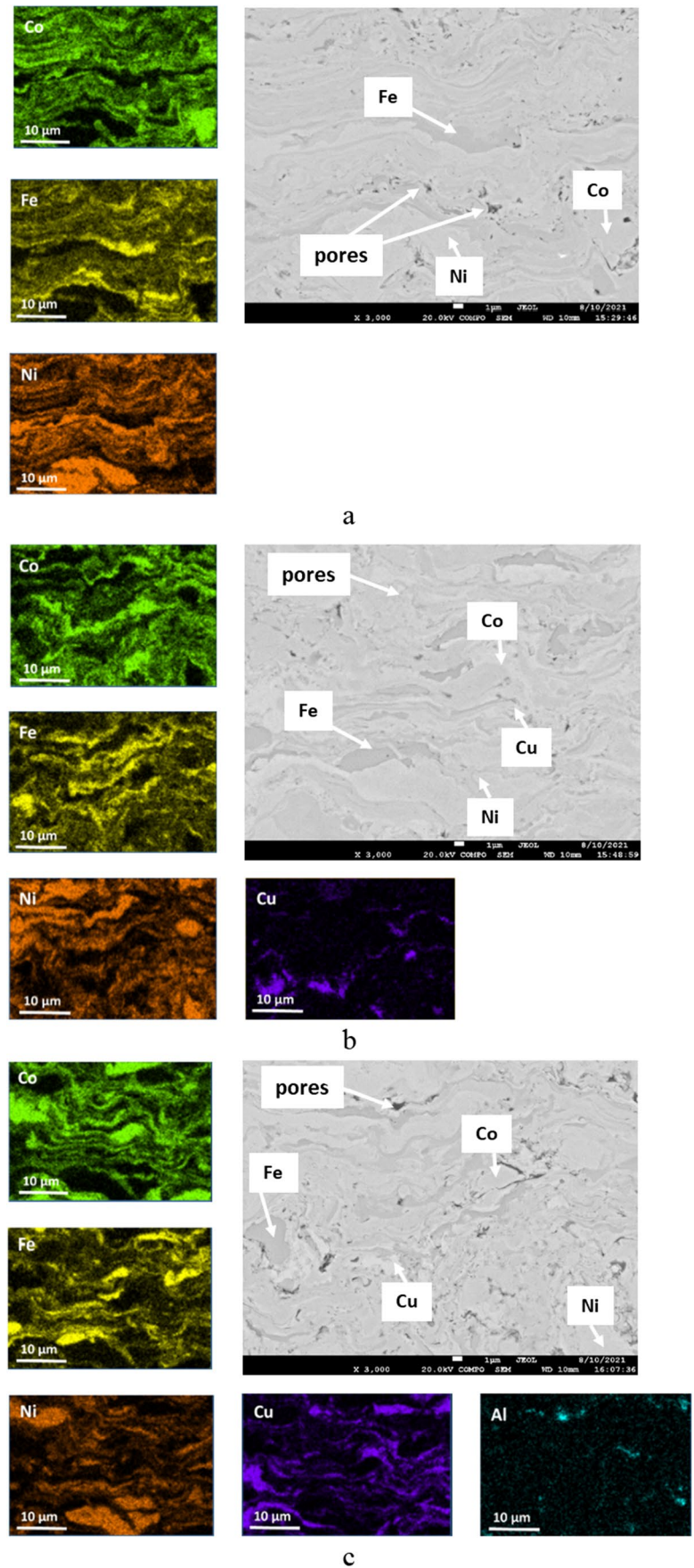
The coating heat treatment of all three precursor coatings was successfully performed. Visual inspection of the samples revealed that the coatings preserved the integrity.

The microstructure and the EDX analysis of the mix I coating after heat treatments are shown in Fig. 8a. The material diffusion enhanced during heat treatment allowed formation of homogeneous structure. In contrast to as-sprayed coatings, the interface between particles is significantly less pronounced. At the same time, some spherical pores with trapped gas were formed in the heat-treated material. The EDS maps also presented in Fig. 8a showed remarkable difference between the distributions of elements in as-sprayed and heat-treated coatings. In particular, significantly more uniform element distribution was observed after heat treatment. The diffusion of Fe, Ni, and Co atoms allowed formation of an alloyed structure in contrast to composite structure of initial coating. At the same time, some local clusters rich in iron, cobalt, or nickel are still visible in the coating, especially in the coating heat treated at 800 °C.

The microstructure observation and element mapping of Mix II coating after heat treatment (Fig. 9) revealed the similar phenomena. However, in contrast to the mix I coating, the influence of heat treatment temperature on the uniformity of element distribution was significantly more pronounced. In particular, the diffusion of copper in the alloy was significantly more pronounced in case of HT at 900 °C than at 800 °C. At the same time, variation of temperature practically did not affect the diffusion of nickel, iron, and cobalt. Also, significant amount of small-scale pores was found.

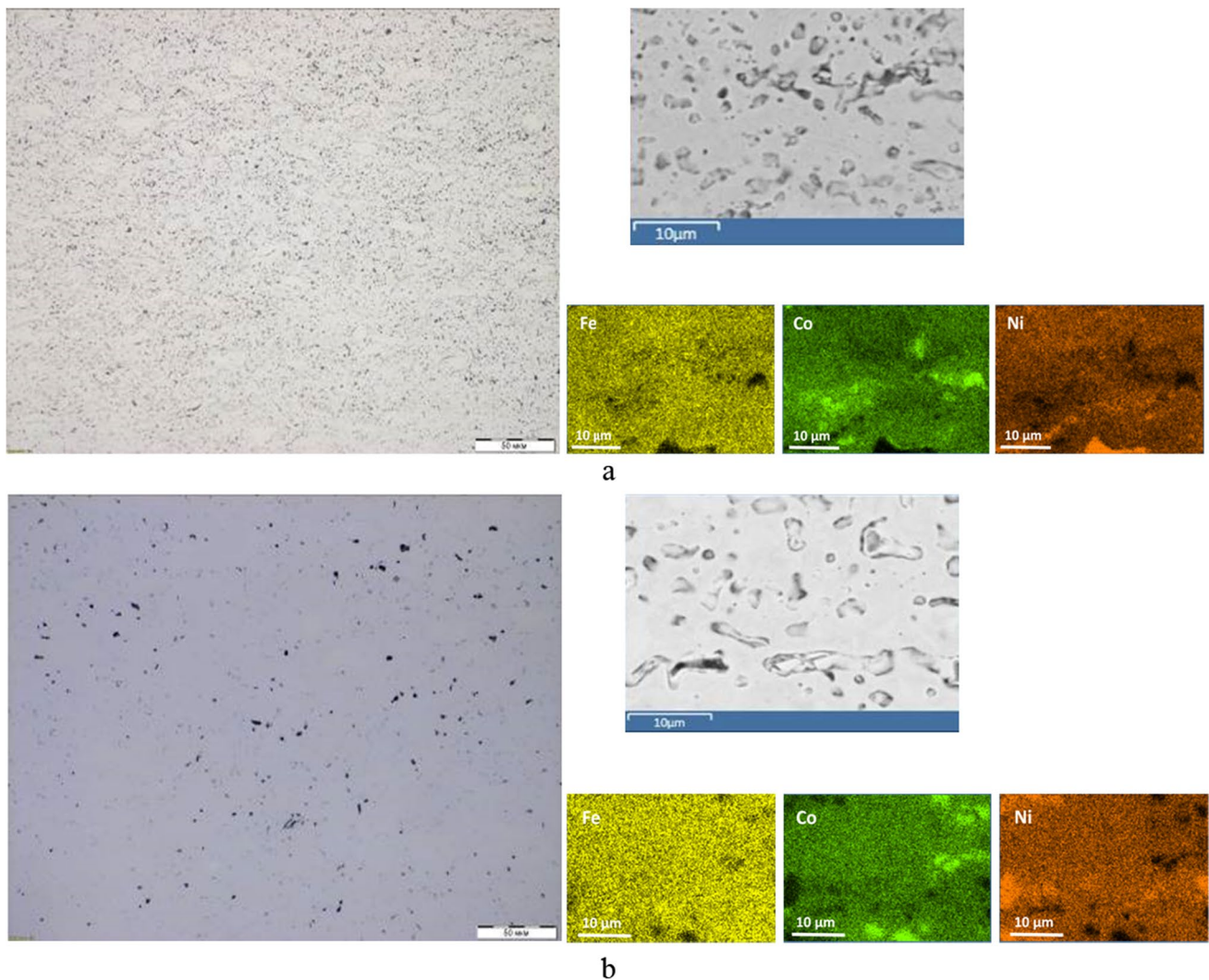
The microstructure and the mapping of elements of the mix III coating after heat treatment is shown in Fig. 10. Again, as well as in the case of mix I and mix II coatings, the element diffusion in mix III allowed formation of alloy structure instead of one composite for both heat-treatment

**Fig. 7** Microstructure and elements mapping of the as-sprayed coatings; **a** Mix I; **b** mix II; **c** mix III



**Table 3** Elemental composition of the composite coatings deposited using powder mixtures; measurements performed by EDS

	Mix I 33% Fe+33% Co+ 33% Ni (atomic percent)	Mix II 25% Fe+25% Co+ 25% Ni+25% Cu (atomic percent)	Mix III 30% Fe+30% Co+30% Ni+ 8% Cu+2% Al (atomic percent)
Al, at.%	0	0	1.4 ± 0.1
Co, at.%	34.5 ± 1.2	29.6 ± 1.4	29.5 ± 1.5
Cu, at.%	0	24.7 ± 1.0	10.4 ± 0.5
Fe, at.%	29.4 ± 1.5	19.1 ± 1.5	25.7 ± 1.5
Ni, at.%	36.1 ± 1.0	26.5 ± 1.3	33 ± 1.0
Enthalpy $\Delta H_{\text{mix}}$ , kJ/mol	-2.51	9.25	1.61
Entropy $\Delta S_{\text{mix}}$ , kJ/mol	9.1	11.42	11.39
Atomic size mismatch $\delta$ , %	0.32	1.11	1.9

**Fig. 8** Microstructure and elements mapping in the mix I coating after heat treatment at 800 °C (a) and 900 °C (b)

temperatures. It should be noted that besides low initial percentage in coating, aluminum diffused in the whole volume of the alloyed material and its distribution became significantly

more uniform. However, some local clusters rich in cobalt, nickel, and copper are present in heat-treated coatings that indicate on insufficient diffusion in some local zones.



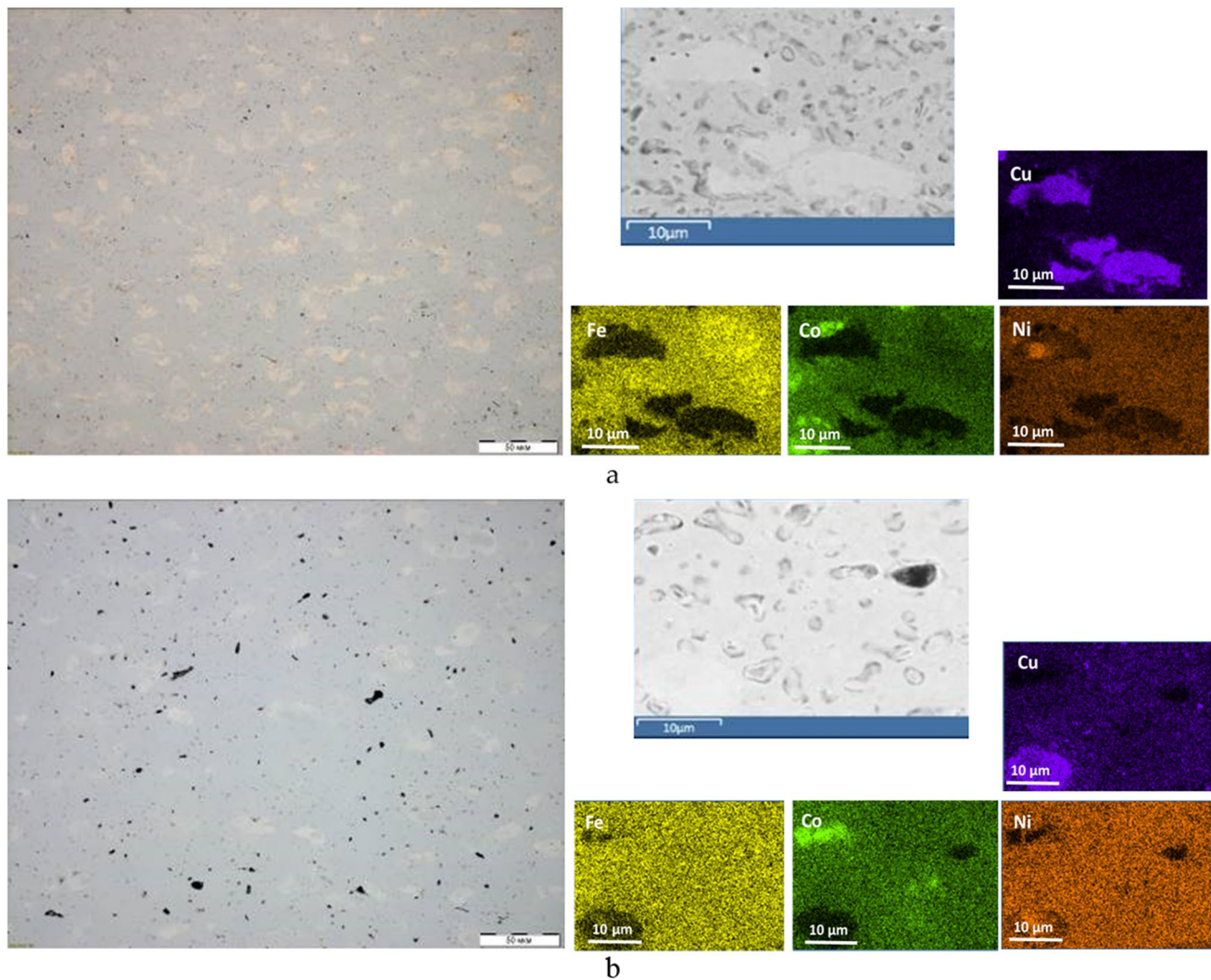


**Fig. 9** Microstructure and elements mapping in the mix II coating after heat treatment at 800 °C (a) and 900 °C (b)

### 3.3 Phase composition and microhardness

Taking into account that the main purpose of the work was to study the possibility of formation of new phases in the composite coatings after heat treatment, the phase analysis by X-ray diffraction method was carried out. The patterns of X-ray diffraction spectrum obtained for as-sprayed and heat-treated coatings are shown in Fig. 11. The asymmetrical peaks observed in the pattern of as-sprayed mix I coating indicate on the start of formation of solid solutions between cobalt, iron, and nickel. Thus, besides relatively short time in molten state (less than 100 μs [13]), slight material diffusion at particle impact allows formation of new *fcc* phase at the particle-particles interface. In contrast mix I, the peaks of metallic copper are detected in the XRD patterns of the as-sprayed mix 2 and mix 3 coatings. One can conclude that the diffusion of copper during impact was less pronounced than the diffusion of other components, and a significant amount

of copper did not participate in the formation of solid solution. Also, the presence of aluminum was not detected in as-sprayed mix III coating probably due to its low percentage.

After heat treatments at 800 °C in all three cases, the formation of single phase with *fcc* structure was observed that resulted in the detection of narrow symmetric peaks in XRD patterns. Increase of heat-treatment temperature up to 900 °C did not change neither the position of the peaks nor its width that indicates on the similar phase composition.

The measurement of coating microhardness is presented in Table 4. One can see that all as-sprayed coatings had the microhardness superior to 400 HV<sub>0.3</sub>. High microhardness value is generally explained by small grain size of deposited material after detonation spraying [21, 22]. Slightly lower value of microhardness of as-sprayed mix II coating in comparison with mix I and mix III is explained by high amount of copper.

Coating heat treatment drastically decreased the coating hardness of coatings mix I and mix II due to formation of

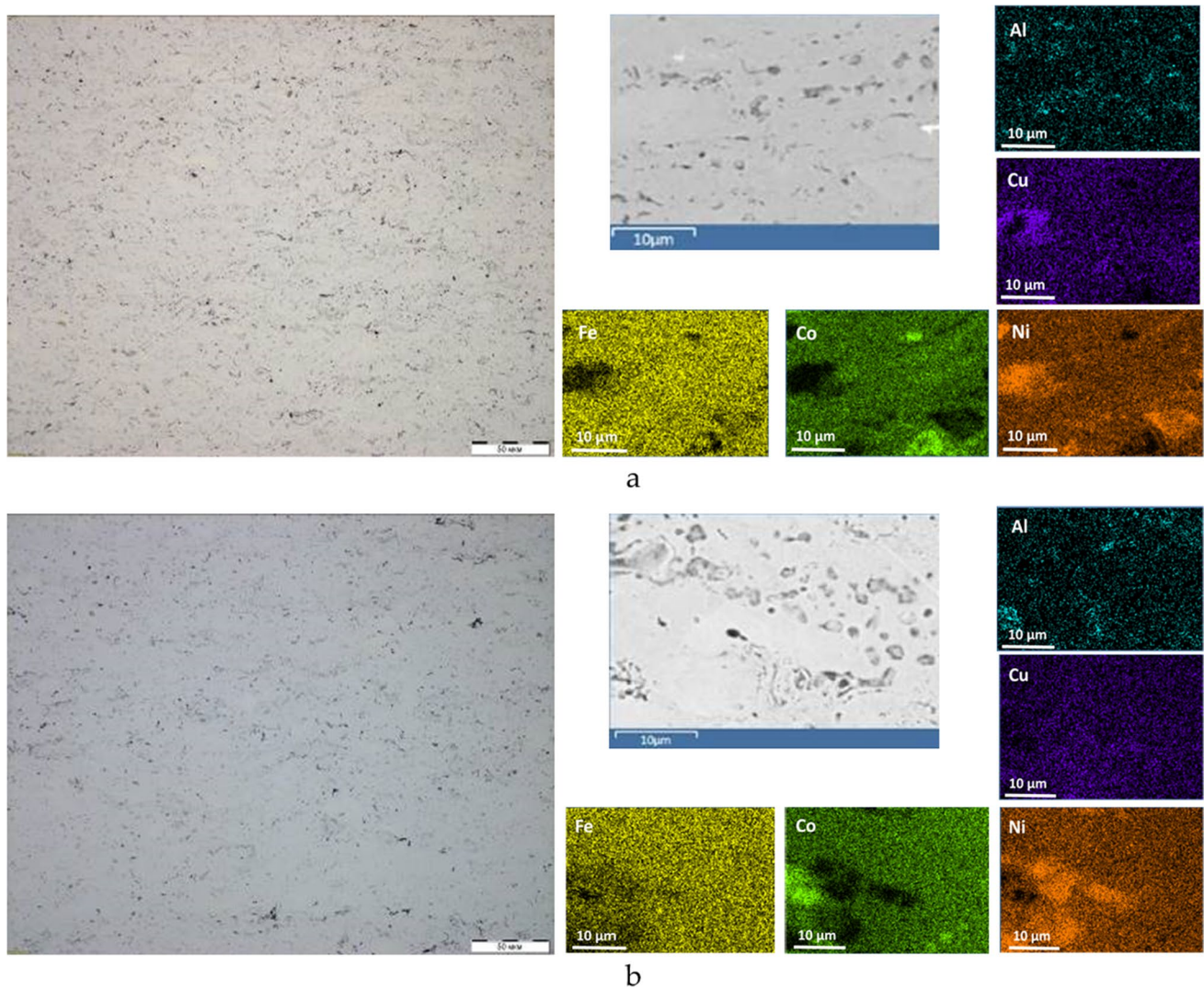


**Fig. 10** Microstructure and elements mapping in the mix III coating after heat treatment at 800 °C (a) and 900 °C (b)

new *fcc* phase and probably due to higher grain size. The addition of aluminum increases the hardness of mix III coatings after heat treatment due to formation of *fcc* structure containing the atoms of aluminum [1].

#### 4 Discussion

The experiments showed that the combination of detonation spraying and heat treatment could be used for elaboration of uniform coating with the composition close to the requirements for high-entropy alloys (case of mix III coating). The coatings preserved its integrity during deposition process and heat treatments. However, for further successful development of this hybrid approach, several important issues should be addressed.

In the approach proposed in this work, the composite precursor coatings were deposited by detonation spraying of mixtures of single-element metal powders. However, possible deviations of coating composition relatively to the initial mixture composition should be taken into account. In our previous work [12], it was shown that the probability of particle bonding to the surface depends not only on the detonation spraying process parameters, but also on the percentage of each component in the mixture. In case of deposition of precursor coating for further synthesis of HEA, even a slight modification of the element percentage from the targeted one could impact the conditions for formation of single solid solution. Thus, the coating composition should be accurately controlled.

It was also found that the spatial structure of the composite influences on the efficiency of elemental diffusion. In current work, the value of characteristic distance  $L$  was

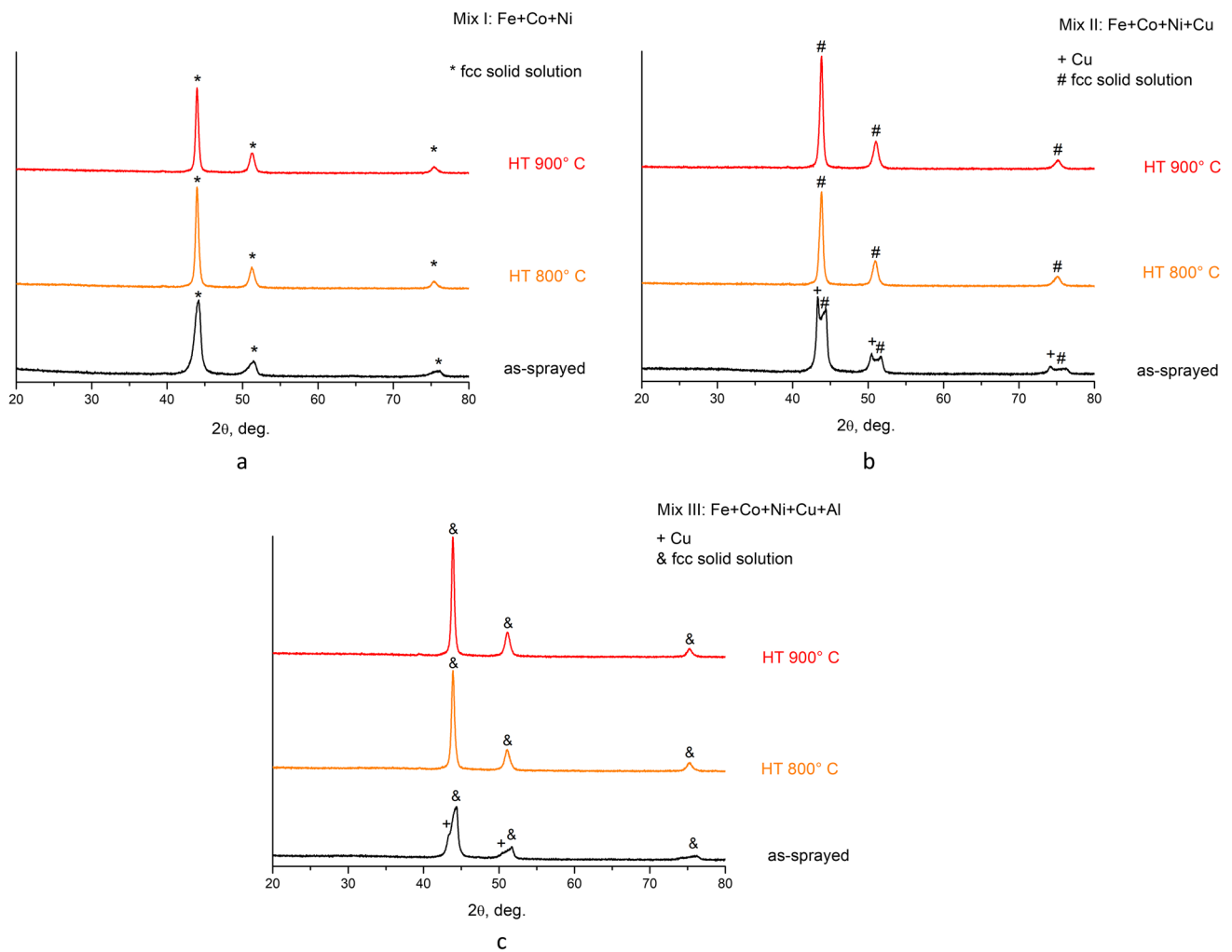


**Fig. 11** Comparison of the X-ray diffraction patterns of the as-sprayed and heat-treated coatings obtained for mix I (a), mix II (b), and mix III (c) coatings

**Table 4** Microhardness of the coating in as-sprayed and heat-treated conditions

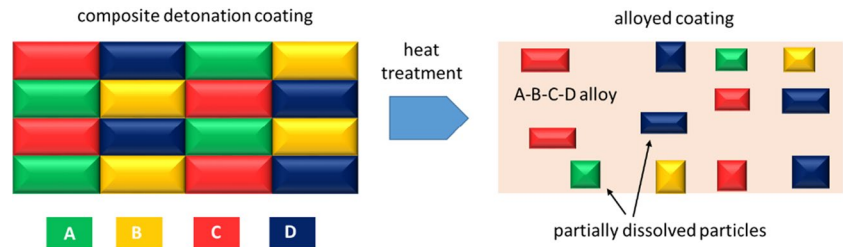
Coating	State	HV <sub>0.3</sub>
Mix I	As-sprayed	486 ± 15
	HT 800 °C	98 ± 5
	HT 900 °C	73 ± 3
Mix II	As-sprayed	408 ± 24
	HT 800 °C	81 ± 5
	HT 900 °C.	82 ± 4
Mix III	As-sprayed	469 ± 17
	HT 800 °C	232 ± 19
	HT 900 °C	150 ± 20

in the range between 10 and 50 μm for mixes I and II and between 10 and 100 μm for mix III. Insufficient particle dissolving during heat treatment and high value of *L* lead to creating of zones richer in some elements than in the other zones. As a result, the formation of coating combining the HEA phase matrix and other phases could be expected (Fig. 12).

To avoid such effect, the powders with smaller granulometry allowing formation of precursors of finer structure with lower characteristic distance *L* between the inclusions could be considered.

Increase of heat-treatment temperature and duration could also enhance the elemental diffusion and improve the

**Fig. 12** Schematics of the influence of insufficient material diffusion on the coating structure after heat treatment



coating uniformity. In the current case, the heat-treatment temperatures were closed to the recrystallization temperature of main elements forming the coatings. However, the difference between the melting points of the composite coating could be a limiting factor significantly reducing the applicable heat-treatment temperature range. In this study, the heat treatment was carried out in solid state for mix I and mix II coatings, whereas the mix III coating treatment was done in solid-liquid state due to the melting of aluminum particles. The low percentage of aluminum in mix III coating did not lead to coating damage during heat treatment. However, the increase of aluminum percentage or addition of another low melting point element to the alloy composition could be a critical factor influencing the coating integrity.

Another important issue that has to be taken into account is the elemental diffusion from the substrate to coating during heat treatment (Fig. 13). The analysis of this phenomenon is not the aim of this study. The results of the coating structure analysis presented above were obtained in the zone located at 150–200  $\mu\text{m}$  from the coating/substrate interface in order to exclude the influence of the substrate. However, in general case, the diffusion of elements from substrate to the coating could modify the elemental composition of the alloy. The thickness of this affected zone could be controlled by optimization of heat-treatment parameters and the refining of the composite structure. In other words, the temperature and the duration of heat treatment should be sufficient for rapid diffusion of elements in the precursor coating but not sufficient for intensive migration of elements

from the substrate to the coating. Thus, the characteristic distance  $L$  should be significantly lower than the mean coating thickness. In this case, the time of heat treatment could be reduced and the depth of the zone affected by diffusion from the substrate will be small.

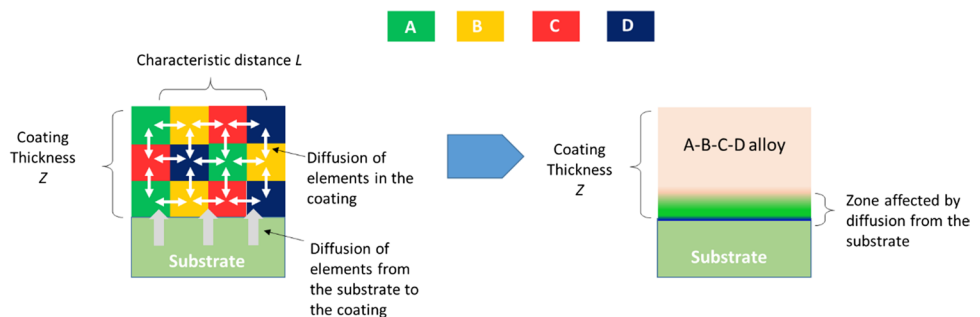
## 5 Conclusions

The feasibility tests of elaboration of high entropy alloy coatings using two-stage approach detonation spraying plus heat treatment were performed. The elemental composition of detonation coatings deposited at the first stage slightly differed from the powder mixture composition. Nevertheless, the coatings had uniform and low-porous structure that was the necessary condition for efficient material diffusion during heat treatment.

Heat treatment applied at the second stage allowed dissolving of composite structure of the coatings due to intensive diffusion of elements. An alloyed coating layer with uniform structure was formed. In all cases, the X-ray diffraction analysis indicated on the formation of alloys with uniform *fcc* structure in heat-treated material.

It is possible to state that the concept of two-stage approach was validated. In future studies, the possibility to deposit the composite with finer initial structure should be analyzed. The optimization of coating heat treatment also could be carried out.

**Fig. 13** Schematics of the influence of diffusion from the substrate on the coating structure during and after heat treatment.



**Author contributions** Igor Batraev: experimental investigation, numerical simulation, methodology, formal analysis

Dina Dudina: experimental investigation, methodology.

Denis Rybin: experimental investigation, numerical simulation, methodology, formal analysis

Vladimir Ulianitsky: conceptualization, methodology, formal analysis, supervision

Alexey Sova: conceptualization, methodology, formal analysis, writing — original draft

Maria Doubeskaia: methodology, formal analysis

Ahmad Ostovari Moghaddam: experimental investigation, formal analysis

Evgeny Trofimov: conceptualization, methodology, formal analysis

Marina Samodurova: conceptualization, methodology, supervision, funding acquisition.

**Funding** This work was supported by the Russian Science Foundation (project No. 20-19-00304).

**Data availability** The authors declare that all data supporting the findings of this study are available within the article. No supplementary data are available.

**Code availability** The LIH code used for simulation is not available for free downloading. The demands should be addressed to Vladimir Yu. Ulianitsky, ulianv@mail.ru.

## Declarations

**Ethics approval** Not applicable.

**Consent to participate** Not applicable.

**Consent for publication** Not applicable.

**Competing interests** The authors declare no competing interests.

## References

- Murty S, Yeh JW, Ranganathan S, Bhattacharjee PP (2019) High-entropy alloys. Elsevier, Amsterdam
- Gorsse S, Couzinié J-P, Miracle DB, From high-entropy alloys to complex concentrated alloys (2018) *Comptes. Rendus Physique* 19(8):721–736
- Silvello A, Torres DE, Rúa RE, Garcia Cano I (2023) Microstructural, mechanical and wear properties of atmospheric plasma-sprayed and high-velocity oxy-fuel AlCoCrFeNi equiatomic high-entropy alloys (HEAs) coatings. *J Therm Spray Technol* 32(2-3):425–442
- Patel P, Alidokht SA, Sharifi N, Roy A, Harrington K, Stoyanov P, Chromik RR, Moreau C (2022) Microstructural and tribological behavior of thermal spray CrMnFeCoNi high entropy alloy coatings. *J. Therm. Spray Technol* 31(4):1285–1301
- Wang H, Kang J, Yue W, Jin G, Li R, Zhou Y, Liang J, Yang Y (2023) Microstructure and corrosive wear properties of CoCrFeNiMn high-entropy alloy coatings. *Materials* 16(1):55. <https://doi.org/10.3390/ma16010055>
- Srivastava M, Jadhav MS, Chethan, Chakradhar RPS, Singh S (2022) Investigation of HVOF sprayed novel Al<sub>1.4</sub>Co<sub>2.1</sub>Cr<sub>0.7</sub>Ni<sub>2.45</sub>Si<sub>0.2</sub>Ti<sub>0.14</sub> HEA coating as bond coat material in TBC system. *J Alloys Compd* 924:166388. <https://doi.org/10.1016/j.jallcom.2022.166388>
- Zhang X, Zhang N, Xing B, Deng C, Wang C (2023) Oxidation behavior of AlCoCrFeNiSix high entropy alloy bond coatings prepared by atmospheric plasma spray. *Surf Coat Technol* 462:129489. <https://doi.org/10.1016/j.surfcoat.2023.129489>
- Kumar H, Bhaduri GA, Manikandan SGK, Kamaraj M, Shiva S (2023) Effect of laser surface processing on the microstructure evolution and multiscale properties of atmospheric plasma sprayed high-entropy alloys coating. *J Therm. Spray Technol* 32(4):831–850
- Wang YM, Xie L, Wu XL, Li CL, Zhou P (2023) Microstructure and tribological properties of FeCoCrNi high-entropy alloy coatings fabricated by atmospheric plasma spraying. *J Mater Eng Perform* 32(8):3475–3486
- Ulianitsky VY, Korchagin MA, Gavrilov AI, Batraev IS, Rybin DK, Ukhina AV, Dudina DV, Samodurova MN, Trofimov EA (2022) FeCoNiCu alloys obtained by detonation spraying and spark plasma sintering of high-energy ball-milled powders. *J Therm Spray Technol* 31(4):1067–1075
- Klenam D, Asumadu T, Bodunrin M, Vandadi M, Bond T, van der Merwe J, Rahbar N, Soboyejo W (2023) Cold spray coatings of complex concentrated alloys: critical assessment of milestones, challenges, and opportunities. *Coatings* 13(3):538. <https://doi.org/10.3390/coatings13030538>
- Ulianitsky VY, Rybin DK, Sova A, Ostovari Moghaddam A, Samodurova M, Doubenskaia M, Trofimov E (2021) Formation of metal composites by detonation spray of powder mixtures. *Int J Adv Manuf Technol* 117(1-2):81–95
- Ulianitsky V, Shtertser A, Zlobin S, Smurov I (2011) Computer-controlled detonation spraying: from process fundamentals toward advanced applications. *J Therm Spray Technol* 20(4):791–801
- Zhang Y, Zhou YJ, Lin JP, Chen GL, Liaw PK (2008) Solid-solution phase formation rules for multi-component alloys. *Adv Eng Mater* 10(6):534–538
- Guo S, Liu CT (2011) Phase stability in high entropy alloys: formation of solid-solution phase or amorphous phase. *Prog Nat Sci: Mater Int* 21(6):433–446
- Xiao DH, Zhou PF, Wu WQ, Diao HY, Gao MC, Song M, Liaw PK (2017) Microstructure, mechanical and corrosion behaviors of AlCoCuFeNi-(Cr,Ti) high entropy alloys. *Mater Des* 116:438–447
- Fu A, Cao Y, Xie Z, Wang J, Liu B (2023) Microstructure and mechanical properties of Al-Fe-Co-Cr-Ni high entropy alloy fabricated via powder extrusion. *J Alloy Compd* 943:169052. <https://doi.org/10.1016/j.jallcom.2023.169052>
- Lim KR, Kwon HJ, Kang J-H, Won JW, Na YS (2020) A novel ultra-high-strength duplex Al–Co–Cr–Fe–Ni high-entropy alloy reinforced with body-centered-cubic ordered-phase particles. *Mater Sci Eng A* 771:138638. <https://doi.org/10.1016/j.msea.2019.138638>
- Kalyankar V, Bhoskar A, Deshmukh D, Patil S (2022) On the performance of metallurgical behaviour of Stellite 6 cladding deposited on SS316L substrate with PTAW process. *Can Metall Quart* 61(2):130–144
- Kalyankar V, Bhoskar A (2021) Influence of torch oscillation on the microstructure of Colmonoy 6 overlay deposition on SS304 substrate with PTA welding process. *Metall Res Technol* 118(4):2021045. <https://doi.org/10.1051/metal/2021045>
- Fauchais PL, Heberlein JVR, Boulos MI (2014) *Thermal spray fundamentals: from powder to part*. Springer, New York
- Pawlowski L (2008) *The science and engineering of thermal spray coatings: Second edition*. John Wiley & Sons

**Publisher's note** Springer Nature remains neutral with regard to jurisdictional claims in published maps and institutional affiliations.

Springer Nature or its licensor (e.g. a society or other partner) holds exclusive rights to this article under a publishing agreement with the author(s) or other rightsholder(s); author self-archiving of the accepted manuscript version of this article is solely governed by the terms of such publishing agreement and applicable law.